

Force Modeling and State Propagation for Navigation and Maneuver Planning for CubeSat Rendezvous, Proximity Operations, and Docking

Christopher W. T. Roscoe, Jacob D. Griesbach, Jason J. Westphal, Dean R. Hawes, and John P. Carrico, Jr.

Applied Defense Solutions, Columbia, Maryland

ABSTRACT

The state propagation accuracy resulting from different choices of gravitational force models and orbital perturbations is investigated for a pair of CubeSats flying in formation in low Earth orbit (LEO). Accurate on-board state propagation is necessary to autonomously plan maneuvers and perform proximity operations and docking safely. The primary perturbations affecting both absolute and relative orbital dynamics in LEO are expected to be J_2 and drag. However, the effect of drag on the relative dynamics is highly dependent on differences in the ballistic coefficients of the two spacecraft, differences which can be large since the CubeSats are non-symmetric in terms of cross-sectional area for different attitudes. Propagation accuracy is investigated both in terms of the absolute (chief) state and the relative (deputy relative to chief) state. Different perturbing effects are normalized and compared on an order of magnitude basis over a wide range of altitudes and inclinations in LEO, and in detail for a 425 km Sun-synchronous orbit.

1. INTRODUCTION

The Proximity Operations Nano-Satellite Flight Demonstration (PONSFD) program will demonstrate rendezvous proximity operations (RPO), formation flying, and docking with a pair of 3U CubeSats. The program is sponsored by NASA Ames via the Office of the Chief Technologist (OCT) in support of its Small Spacecraft Technology Program (SSTP). The goal of the mission is to demonstrate complex RPO and docking operations with a pair of low-cost 3U CubeSat satellites using passive navigation sensors, and it is expected to fly in low Earth orbit (LEO) with an altitude of 400 km–700 km. The ability to accurately perform state propagation on-board is necessary to plan maneuvers and long-term spacecraft trajectories without incurring unnecessary fuel cost and to perform proximity operations and docking of the two spacecraft safely. This paper deals with the problem of performing precision on-board navigation and maneuver planning with limited computer processing power, while placing emphasis on spacecraft autonomy. This problem actually has two aspects, the choice of force model and the method of numerical integration, but the present paper will focus on the first one.

The question of which force model components will dominate in a given orbit regime has been an important consideration for astrodynamists since the beginning of the space age. In 1959, Brouwer [1] introduced the notion of mean orbital elements and solved the problem of motion about an oblate spheroid using Hamiltonian mechanics and the method of averaging for the first five zonal harmonics of the Earth. As improved models of the geopotential became available and other perturbations gained importance, Brouwer theory formed the basis for a number of semianalytical ephemeris theories which used mean elements but incorporated higher-order gravity terms and some additional perturbations. In 1996, Barker [2] studied the effects of truncating different geopotential models to estimate an error budget for a variety of orbit categories for the Space Defense Operations Center (SPADOC) space surveillance mission. This study evaluated propagation error in terms of orbit determination (OD) and final predicted position compared to actual observations, and it suggested that the truncation of zonal terms had more of an impact on accuracy than the truncation of the tesseral and sectorial terms. In 2003, Register [3] compared the contributions of individual forces to orbit determination accuracy, including central body, higher-order geopotential, atmospheric drag, lunar and solar third-body perturbations (TBP), solar radiation pressure (SRP), solid Earth tide, and others.

A more comprehensive analysis was performed by Vallado [4] in 2005, which examined the variation of position accuracy over time, rather than only final position accuracy, for a number of force model contributions. This study found that in lower LEO (the expected orbit regime for PONSFD) the primary orbital perturbation is, in general, the Earth oblateness, or J_2 , perturbation, followed by atmospheric drag and higher-order geopotential terms. Beyond geopotential degree and order of about 12×12 , it becomes harder to draw general conclusions since higher-order gravity terms, TBP, and SRP can all have similar effects on propagation accuracy, depending on the specific orbit considered. In addition, the accuracy is very sensitive to modeling errors, especially parameters affecting atmospheric

drag. This analysis also confirmed the importance of the higher-order zonal terms in the geopotential by examining sensitivities for both square and non-square gravity model truncations. As was noted by Barker [2], larger square gravity field sizes do not always imply a more accurate solution, due to the fact that the neglected higher-order terms do not always have smaller magnitudes than the included lower-order terms (examples for additional satellites can be found in [5]). Unfortunately, a general conclusion as to the “best” gravity model truncation is not possible because, as with the smaller perturbations, the accuracy depends on the specific orbit considered.

The effects of atmospheric drag are extremely challenging to predict accurately because of difficulties in determining atmospheric density, modeling interactions between the atmosphere and the satellite surface, and uncertain knowledge of a satellite’s attitude. The first two of these issues were investigated in detail by Vallado and Finkleman [6], who demonstrated just how much of an impact drag modeling choices can have on propagation accuracy. In fact, modeling errors in this area can have a much greater effect than many of the smaller orbital perturbations described above, and this will be an important consideration when selecting a force model for use in the PONSFD guidance and navigation system. For spacecraft formations, where relative dynamics and not absolute dynamics are of primary importance, drag effects become highly dependent on differences in the ballistic coefficients of the spacecraft in the formation.

The subject of force modeling for high-precision navigation of satellite formations has been addressed in the literature mainly by numerical analysis because of the difficulty in drawing general conclusions when accuracy is primarily dependent on specific orbit parameters and mission characteristics. Carpenter and Alfriend [7] presented some guidelines on relative navigation accuracy required for performing maneuvers and demonstrated that differential semimajor axis uncertainty is usually the most important error in formation flying, but this analysis did not account for non-two-body perturbations. Sabol et al. [8] investigated the effects of different perturbations on propagation accuracy and formation stability using mean elements and semianalytical techniques. Wnuk and Golebiewska [9] did a similar analysis using numerical integration, but they neglected the effects of atmospheric drag, which is of primary importance in lower LEO. Romanelli et al. [10] compared the maximum differential disturbing accelerations due to J_2 – J_6 , atmospheric drag, and SRP for spacecraft flying in close formations from LEO to geostationary Earth orbit (GEO) to determine what magnitude of control force would be required for formation-keeping. Hughes [11] performed a perturbation sensitivity analysis for the MMS mission, which is a high-altitude, high-eccentricity formation flying mission. Roscoe et al. [12] looked in-depth at the effects of the lunar perturbation on that mission and compared them to the effects of J_2 , but as PONSFD will fly in a very different orbit regime the results are not directly applicable. In LEO, D’Amico et al. [13] investigated force model selection for the navigation system of the PRISMA mission, which used differential carrier-phase GPS for precision relative navigation. However, we expect our conclusions to be different since PONSFD uses direct relative measurements.

This paper investigates the accuracy of performing long-term state propagation using different choices of gravitational force models and orbital perturbations for a range of orbit altitude and inclination possibilities in lower LEO. Propagation accuracy is investigated both in terms of the absolute (chief) state and the relative (deputy relative to chief) state. Propagation accuracy is affected by a number of orbit and force model parameters which makes performing such a study with uncertain orbit knowledge a challenging prospect. However, much intuition can be gained by breaking the study down in terms of each of these parameters to see the effect of each one individually. Different perturbing effects are normalized and compared on an order of magnitude basis over a wide range of altitudes and inclinations in LEO, and in detail for a 425 km Sun-synchronous orbit, which is the current baseline for PONSFD. The results of this study will be used to select a propagation method for the on-board navigation system for the mission.

2. DYNAMIC MODEL

The motion of a satellite in Earth orbit is governed by the vector differential equation,

$$\ddot{\mathbf{R}} = -\frac{\mu}{R^3}\mathbf{R} + \mathbf{f}_{\text{pert}} \quad (1)$$

where \mathbf{R} is its position with respect to the center of the Earth, R is the magnitude of that position, μ is the geocentric gravitational constant, $(\dot{})$ indicates differentiation with respect to an inertial reference frame, and \mathbf{f}_{pert} represents any perturbations to the two-body motion. As is common in astrodynamics, in this paper forces are written as per unit mass (accelerations). The two-body part of the motion can be solved in a straightforward manner, but we cannot, in

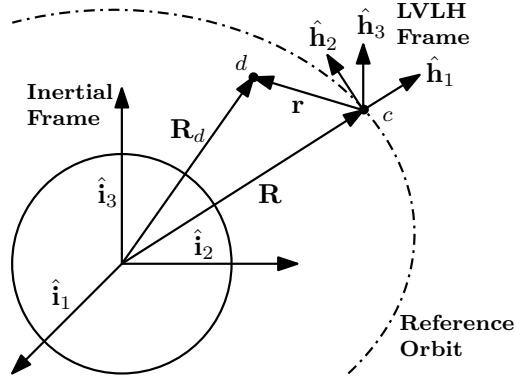


Fig. 1. Local-vertical–local-horizontal reference frame.

general, find analytical solutions for motion due to arbitrary perturbation forces. In this analysis we will focus on perturbations due to the asphericity of the Earth, atmospheric drag, lunar and solar TBP, and SRP.

Since this paper deals with a pair of spacecraft flying in formation, we need some additional definitions. One of the spacecraft is designated the “chief” and its motion defines the “absolute” or reference trajectory of the formation. The second spacecraft is designated the “deputy” and we describe its motion relative to the chief as the “relative” trajectory. The relative motion is expressed in the local-vertical–local-horizontal (LVLH) reference frame, as depicted in Figure 1. The location of the chief defines the origin of this frame and \hat{h}_1 is in the direction of its orbit radius, \hat{h}_3 is in the direction of its angular momentum, and \hat{h}_2 completes the right-hand coordinate system. In this paper, the perturbed absolute trajectories of each spacecraft are integrated separately and the relative motion is calculated at each time step in the instantaneous LVLH reference frame.

2.1 Non-Spherical Earth Gravity

The most important perturbation in Earth orbit is the effect of the asphericity of the central body. This force is determined through a potential function U . There are several ways to express the potential, but we adopt the definition [5]

$$U = -\frac{\mu}{R} \left[1 - \sum_{k=2}^{\infty} J_k \left(\frac{R_e}{R}\right)^k P_k(\sin \phi) + \sum_{k=2}^{\infty} \sum_{j=1}^k \left(\frac{R_e}{R}\right)^k P_{k,j}(\sin \phi) (C_{k,j} \cos j\lambda + S_{k,j} \sin j\lambda) \right] \quad (2)$$

where the J_k are the zonal harmonics, $C_{k,j}$ are the tesseral harmonics, $S_{k,j}$ are the sectorial harmonics, R_e is the mean equatorial radius of the Earth, P_k are the Legendre polynomials, $P_{k,j}$ are the associated Legendre functions, ϕ is the satellite’s geocentric latitude, and λ is the satellite’s geocentric longitude. This form includes the two-body part of the potential as the first term. A detailed discussion of the harmonic gravity terms can be found in [5]. It is important to note that this series is infinite and not monotonically decreasing, so it is not strictly valid to truncate this series and expect a certain accuracy. Nevertheless, due to computational processing limitations it is common practice to do so, but care must be taken to ensure that dominant terms are retained. The most influential term in this series, by several orders of magnitude, is the J_2 zonal harmonic, which is related to the equatorial bulge of the Earth. In this paper, when we refer to an $m \times n$ gravity field, we mean that k is truncated at m and j is truncated at n , where $n \leq m$.

2.2 Atmospheric Drag

The next most important perturbation in LEO is the effect of atmospheric drag. The basic equation for drag is [5]

$$\mathbf{f}_{\text{drag}} = -\frac{1}{2} \frac{c_D A}{m} \rho V_{\text{rel}} \mathbf{V}_{\text{rel}} \quad (3)$$

where c_D is the satellite’s drag coefficient, A is its exposed cross-sectional area, m is its mass, ρ is the atmospheric density, and \mathbf{V}_{rel} is the velocity of the satellite relative to the atmosphere. As mentioned previously, although Eq. (3)

is simple, the parameters governing the magnitude of the drag force are extremely challenging to predict accurately. These issues are discussed in detail in [6]. For two spacecraft flying in close formation, we can assume that the atmospheric density affecting them and their velocities relative to the atmosphere are approximately the same. Therefore, the most important consideration in formation flying is the difference in their ballistic coefficient β , defined as $m/c_D A$, which, for identical, non-symmetrical spacecraft, is mainly determined by their relative attitude.

2.3 Third-Body Perturbations

Assuming that the mass of the satellite is small relative to the celestial bodies, the disturbing force in Earth orbit due to the gravitational acceleration of a third body is [12]

$$\mathbf{f}_{TBP} = Gm_t \left(\frac{1}{d_t^3} \mathbf{d}_t - \frac{1}{r_t^3} \mathbf{r}_t \right) \quad (4)$$

where G is the universal gravitational constant, m_t is the mass of the third body, \mathbf{d}_t is the position of the third body relative to the satellite, and \mathbf{r}_t is the position of the third body relative to the Earth. The magnitude of this perturbation is proportional to the mass of the third body and inversely proportional to the square of the distance between the satellite and the third body, so it is typically more important for satellites in higher altitude orbits. In this paper, we consider the third-body effects of the Sun and the Moon.

2.4 Solar Radiation Pressure

Solar radiation pressure is expected to be the smaller perturbation considered in this paper, since it mainly effects high-altitude and high area-to-mass ratio satellites. The force due to SRP is [5]

$$\mathbf{f}_{SRP} = -\frac{p_s c_R A_s}{m} \frac{1}{d_s} \mathbf{d}_s \quad (5)$$

where p_s is the solar pressure per unit area, c_R is the satellite's coefficient of reflectivity, A_s is the exposed area to the Sun, and \mathbf{d}_s is the position of the Sun relative to the satellite. As with atmospheric drag, for a pair of identical spacecraft flying in formation, the relative effect of this perturbation will depend on differences in their exposed areas.

3. ORDER OF MAGNITUDE COMPARISON

In this section, we compare the effects of those force model parameters expected to be of primary interest on an order of magnitude basis. Results were obtained for a 10 day time span for both absolute and relative states over altitudes ranging from 400 km–700 km and inclinations ranging from 40°–140°. In all cases, a small eccentricity of 0.005 was used, since the PONSFD orbit is expected to be near-circular, and it was assumed that right ascension of ascending node, argument of perigee, and initial mean anomaly would not have a significant impact on the results, provided the simulations were performed over a sufficiently long time period to average out any Earth-orientation or third-body-geometry specific effects. All simulations were performed using Analytical Graphics, Inc. Systems Tool Kit (STK) with RK78 integration, and the “truth” model included a 70×70 geopotential with atmospheric drag, lunar and solar TBP, SRP, and solid Earth tides. For atmospheric drag computation, the Jacchia-Roberts atmospheric density model was used with predicted $F_{10.7}$ values obtained from the March 2013 NASA Marshall Space Flight Center Future Solar Activity Estimates [14] for January 2015. The nominal cross-sectional area used for the spacecraft was 0.1024 m², which corresponds to the maximum drag configuration.

Absolute and relative ephemerides were computed and compared to the full truth model using different degree and order gravity models (2-body, J_2 -only, and square fields up to 30×30) for 5 different combinations of drag, TBP, and SRP. In each of the cases with drag, two configurations were considered: one with the spacecraft flying parallel to each other (null differential drag), and one with an attitude difference of approximately 45° to give the deputy a cross-sectional area of 0.06 m² compared to the chief's 0.1024 m² (moderate differential drag). This configuration was deemed to be a more realistic possibility than a “worst-case” orientation in which the satellites fly in exactly orthogonal attitudes. In all cases, the spacecraft began in a 20 km leader-follower configuration, which was perturbed slightly with a differential semimajor axis error of 2 m and small errors in each of the remaining differential elements.

Note that the propagation in this section is performed over an extremely long time span—10 days is approximately 150 orbits at these altitudes, which is far longer than we would ever expect to propagate on-board these spacecraft. We do this to allow the perturbation effects to grow very large to highlight the differences in their orders of magnitude. However, as evaluating actual position and velocity error magnitudes in such a case would be highly misleading, we will normalize the propagation results as follows.

3.1 Normalization of Results

Most of the previous force modeling studies focused on position error, but, for formation flying in particular, it is important to consider velocity errors as well because of their significant impact on maneuver targeting. However, over long time spans the perturbations considered in this paper cause significant changes in the orientation of the orbit plane, and the (vector) velocity error tends to mirror the position error because of the large differences in direction between the propagated velocity vector and the true velocity vector. The orientation of a satellite’s orbit is defined by the angles Ω (right ascension of the ascending node), i (inclination), and ω (argument of perigee). Position magnitude and speed, on the other hand, are defined the elements a (semimajor axis), e (eccentricity), and f (true anomaly) through the orbit and vis-viva equations. Note that errors in ω , e and f have very little influence in near-circular orbits. When differences in orientation are large, vector errors in position and velocity are both dominated by errors in Ω , i , and ω , and the effects of errors in the other elements are not captured. Therefore, we consider errors in speed, which are primarily related to errors in semimajor axis for near-circular orbits, instead of velocity in order to capture these different aspects of the propagation accuracy. Relative velocity errors are directly related to differential semimajor axis uncertainty, which, as noted by Carpenter and Alfriend [7], is usually the most important error in formation flying.

In order to combine these errors into a single parameter for comparison over numerous cases, position errors are divided by the Earth’s equatorial radius R_e and speed errors are divided by $V_{e,c}/100$, where $V_{e,c} = \sqrt{\mu/R_e}$ is the circular orbit speed at the equator, and added together to form a normalized error,

$$e_{\text{abs}} = \frac{|\mathbf{R}_i - \mathbf{R}_{\text{truth}}|}{R_e} + \frac{||\mathbf{V}_i| - |\mathbf{V}_{\text{truth}}||}{V_{e,c}/100} \quad (6)$$

where \mathbf{R}_i and \mathbf{V}_i are the absolute position and velocity in the i th case and $\mathbf{R}_{\text{truth}}$ and $\mathbf{V}_{\text{truth}}$ are the position and velocity from the truth model. This normalization was chosen to give approximately equal magnitude influence to position and speed errors over the entire range of results. The relative results are also normalized, but this time LVLH speed errors are divided by $V_{e,c}$ in order to give them approximately the same magnitude as relative position errors:

$$e_{\text{rel}} = \frac{|\mathbf{r}_i - \mathbf{r}_{\text{truth}}|}{R_e} + \frac{||\mathbf{v}_i| - |\mathbf{v}_{\text{truth}}||}{V_{e,c}} \quad (7)$$

\mathbf{r}_i and \mathbf{v}_i are the relative position and (LVLH) velocity in the i th case and $\mathbf{r}_{\text{truth}}$ and $\mathbf{v}_{\text{truth}}$ are the relative position and velocity from the truth model.

Finally, to obtain a single value for comparison, we take the largest value of e_{abs} or e_{rel} throughout the 10 day time span. We call this value the maximum normalized error and it is the basis for the comparisons shown in subsequent sections. Note that in the following plots, “Gravity order/degree n ” refers to a square gravity field of order and degree $n \times n$, except that “0” implies Keplerian, two-body gravity and “1” implies perturbed two-body gravity with J_2 only.

3.2 Third-Body Perturbations and Solar Radiation Pressure

Before examining the full range of results for different altitudes and inclinations, the effects of lunar and solar third-body perturbations and solar radiation pressure are analyzed separately, since they are expected to be small in this orbit regime. Figures 2(a) and (b) show representative results of absolute and relative propagation accuracy for the cases with SRP, TBP, and drag (with moderate differential drag). In all of the simulations, the error in cases with TBP and SRP is almost indistinguishable from the geopotential-only results. Clearly, compared to drag and geopotential effects, TBP and SRP are quite small and likely do not need to be considered for our application. In general, the magnitude of TBP effects were found to be slightly greater than SRP, so an additional case was considered which included both TBP and drag (shown in the same figures), but the conclusion does not change. Therefore, in the following sections, results will only be shown for cases with and without drag, not TBP or SRP.

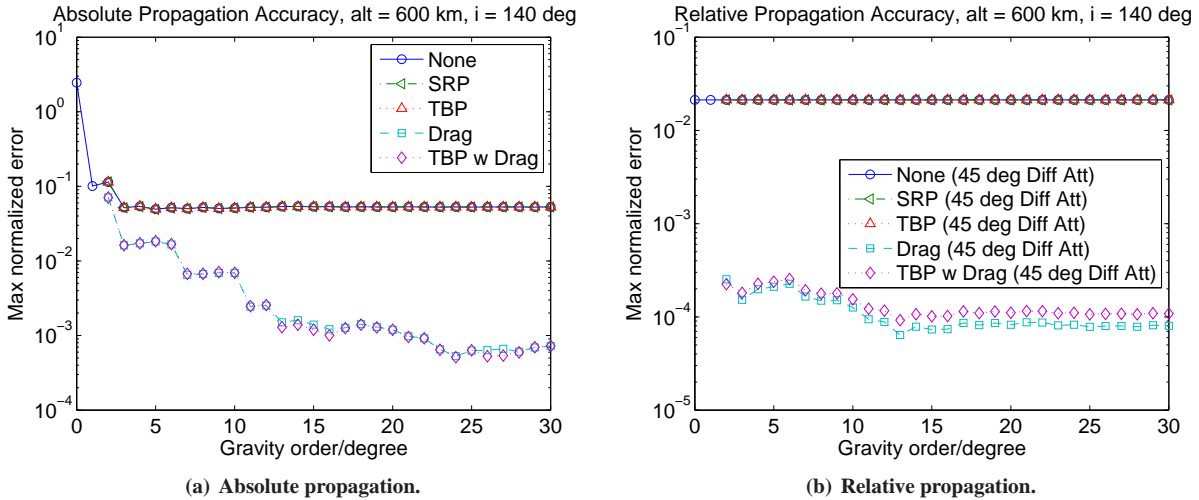


Fig. 2. Typical effects of TBP and SRP compared to drag.

3.3 Full Results

Figure 3 shows the full results of the force model order of magnitude comparison for absolute propagation over different orbit altitudes and inclinations. In this plot, results are grouped by orbit altitude and whether or not drag is included in the force model. Thin lines show the results for individual inclinations at each altitude and thick lines show the results averaged over all inclinations. Several general conclusions can be drawn from this plot:

1. As expected, J_2 is the largest perturbation in all cases.
2. Atmospheric drag is the second-largest perturbation and is comparable to J_2 at lower altitudes.
3. Going from only J_2 to a 2×2 gravity field does not tend to improve the propagation accuracy (and in many cases actually reduced the accuracy), due to the truncation of higher-order zonal terms which are on the same order of magnitude as the included second-degree terms.
4. When drag is not included in the force model, there is little improvement in accuracy for gravity models larger than 3×3 , since the neglected atmospheric drag effects are dominant.

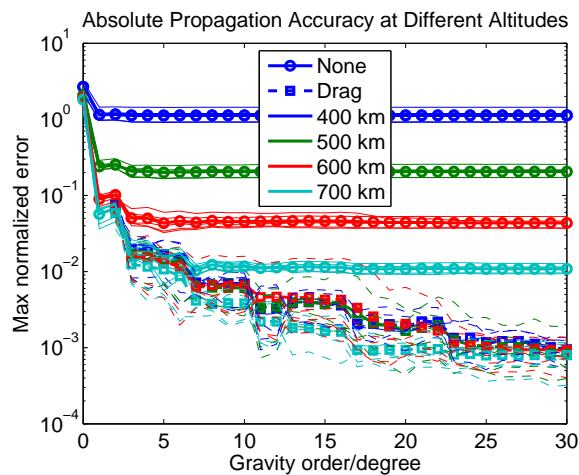


Fig. 3. Full force model order of magnitude comparison for absolute propagation. Thick lines show the averaged results for each altitude (in different colors), over all inclinations, thin lines are the results for specific inclinations, and circles/solid lines and squares/dashed lines indicate propagation without and with drag, respectively.

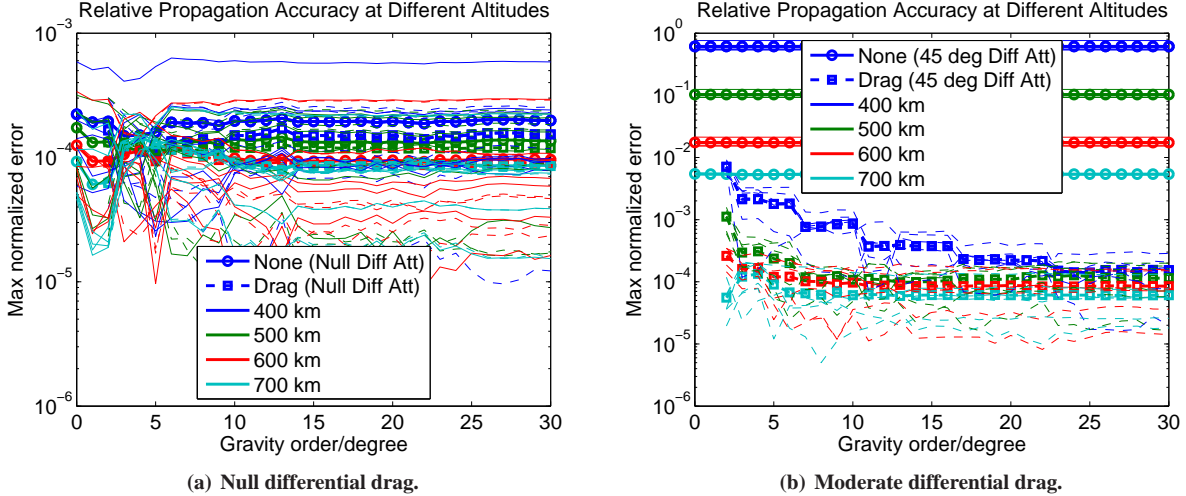


Fig. 4. Full force model order of magnitude comparison for relative propagation. Thick lines show the averaged results for each altitude (in different colors), over all inclinations, thin lines are the results for specific inclinations, and circles/solid lines and squares/dashed lines indicate propagation without and with drag, respectively.

- When drag is included in the force model, there is a general improvement in accuracy for gravity fields of order/degree higher than 2×2 , but the improvement is not monotonic and there is no clear “best” gravity model truncation. This agrees with the observations of Barker et al. [2] and Vallado [4].

In addition, there is a clear correlation between altitude and propagation accuracy when drag is not modeled. This is to be expected, since the magnitude of the atmospheric drag force is proportional to atmospheric density, which is higher at lower altitudes. There is also a strong relationship between orbit inclination and propagation accuracy, with near-polar orbits exhibiting better accuracy than near-equatorial ones. As with the influence of orbit altitude, this is due to the influence of the flattening of the Earth on the apparent altitude of the spacecraft and the greater thickness of the atmosphere near the equator compared to the poles, both of which affect the magnitude of the drag force.

Figures 4(a) and (b) show the full results of the force model order of magnitude comparison for relative propagation for the null and moderate differential drag cases, respectively. As expected, when the spacecraft have the same cross-sectional area, differential drag has very little impact. In addition, higher-order geopotential terms have very little impact, on average, in this case. In the moderate differential drag case, there is virtually no improvement in accuracy with higher-order geopotential terms, or even J_2 , since differential drag effects over such a long time period are very large. When drag is included in the model, there is a general improvement in accuracy with higher order/degree gravity fields, especially at lower altitudes, which shows a clear correlation between geopotential and drag effects in this case. These results indicate that if differential drag is kept to a minimum we could employ a relatively low-order gravity field and not suffer much loss of propagation accuracy, from a relative motion perspective. However, if differential drag is significant, it will be important to use a somewhat higher-order gravity field. The actual choice of gravity field must be investigated further and tailored to the specific flight orbit and mission profile.

4. DETAILED COMPARISON FOR PONSFD ORBIT

The previous section compared order of magnitude for different force modeling errors by propagating for an extremely long time span. In this section, we examine a more realistic (but still stressing) 1 day propagation case, a duration we could reasonably expect to perform on-board. For this analysis, we restrict our attention to a 425 km Sun-synchronous orbit, with an inclination of 97.04° , which is currently being used as the baseline orbit for design of the PONSFD mission. At this altitude, 1 day corresponds to about 15 orbits, and the same perturbed 20 km leader-follower initial conditions are used. In this case, the chief has an attitude about 45° off of the velocity, giving it a cross-sectional area of 0.07 m^2 , and the deputy has an attitude about 55° off of the velocity, giving it a cross-sectional area of 0.06 m^2 .

The results of the previous section suggest that modeling drag is key to accurately propagating the absolute state and is also important for relative propagation if differential drag is not zero. However, this assumes that we have perfect knowledge of atmospheric density (including solar flux), both chief and deputy attitude, and the drag coefficient of the spacecraft (and also assumes that our drag model is realistic). In particular, having perfect knowledge of the deputy attitude will be challenging given the limitations of our on-board sensors and desire not to rely on inter-satellite communications for relaying telemetry. Therefore, in this section we examine the effects of these assumptions by considering four perturbation model cases: (i) No drag; (ii) With drag and perfect atmosphere and attitude knowledge; (iii) With drag and perfect attitude knowledge, but incorrect atmosphere model; and (iv) With drag and perfect atmosphere knowledge, but incorrect attitude estimates of 47° for the chief (0.067 m^2 area) and 10° for the deputy (0.1 m^2 area). In the last case, the chief attitude knowledge is made much better than the deputy attitude knowledge because that will likely be a realistic operational case for on-board propagation.

Figures 5(a) and (b) show the normalized results for the cases described above for absolute and relative propagation, respectively. In the case of the 1 day time span with smaller cross-sectional area, drag effects have not built up as much as in the case of the 10 day time span, so we can now see noticeable improvements in absolute accuracy as gravity degree/order is increased, even in the case where drag is not modeled. As before, however, there is no significant increase in relative accuracy with higher-order gravity when drag is not modeled. In fact, even when drag is modeled (correctly or incorrectly), there is no great difference in accuracy for different geopotential orders, except that models of order and degree from 3×3 to 9×9 perform worse than others when drag is modeled correctly. Note, however, that these differences are very small when compared to the effects of errors in the drag model and would be “in the noise” for our application.

When drag is modeled using the different atmosphere model, there is no longer as great an improvement in either absolute or relative accuracy, even though the attitude is known perfectly. For the incorrect attitude case, the absolute accuracy is almost unchanged, except for very high-order gravity models, which is to be expected since the chief’s attitude knowledge error is very small. The relative accuracy is significantly diminished when the deputy’s attitude knowledge error is large, and in this case is worse than if drag is not modeled at all.

These results clearly demonstrate that if drag is to be included in the force model it is essential to use an accurate atmospheric density model and ensure that accurate attitude information for both spacecraft will be available, as previously discussed by Vallado and Finkleman [6]. For formation flying with identical spacecraft, it is also advantageous to adopt a nominal formation configuration in which the spacecraft fly in parallel to minimize the effects of differential drag on both navigation and formation stability. For PONSFD, this is implied in the mission Concept of Operations, since during proximity operations the spacecraft are to face each other to orient their relative navigation sensors which will give them approximately the same cross-sectional area.

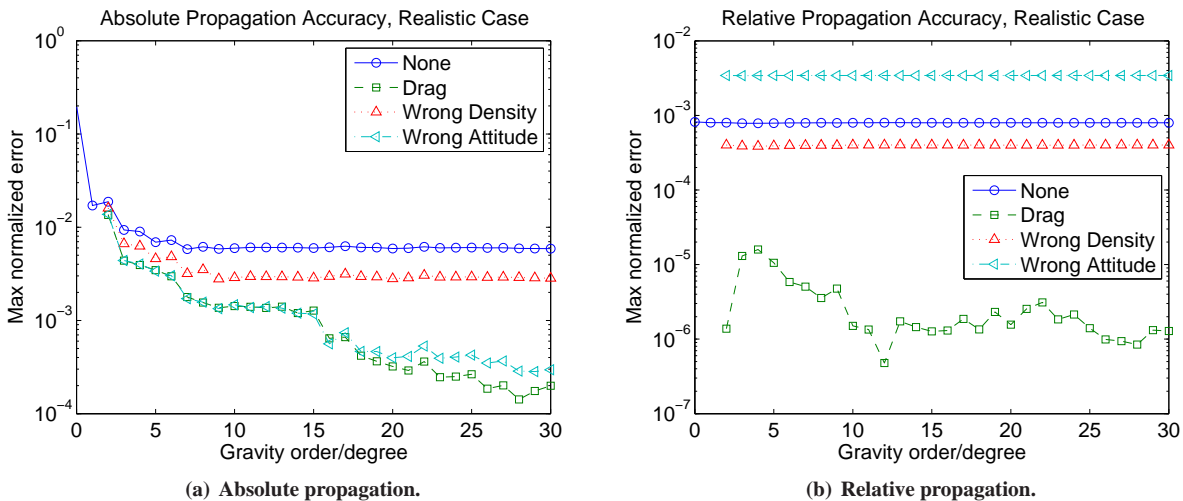


Fig. 5. Comparison of accuracy for realistic on-board propagation case.

4.1 Square vs. Non-Square Gravity Field

Since both Barker [2] and Vallado [4] suggested that truncation of the zonal terms in the geopotential has more of an impact on propagation accuracy than truncation of the tesseral and sectorial terms, we now investigate the effects of using a non-square geopotential on the results of the 1 day, 425 km Sun-synchronous simulation (with perfect drag modeling). Figures 6(a) and (b) show the absolute and relative propagation results, respectively, for different combinations of non-square gravity fields. In each set of results, the tesseral/sectorial degree cannot be greater than the zonal harmonic order, hence the non-square gravity results do not go all the way up to degree 30. For example, the “8th Order Zonal” result only goes up to an 8×8 gravity field, where it intersects with the “Square Potential” result.

From the absolute propagation results, it is clear that the truncation of the zonal terms is indeed more important than the truncation of the tesseral and sectorial terms, particularly for tesseral/sectorial degree less than 9 and greater than 14. However, it appears that the 15th and 16th degree tesseral/sectorial terms are also quite important, for very high accuracy applications. There is more variation in the relative propagation results, since the magnitude of the errors is so much smaller, but the same general conclusion holds that the zonal terms are of primary importance, particularly the 12th order term in this case. (More specifically, one of the terms between 9th and 12th order, since only the 12th order term is shown here.)

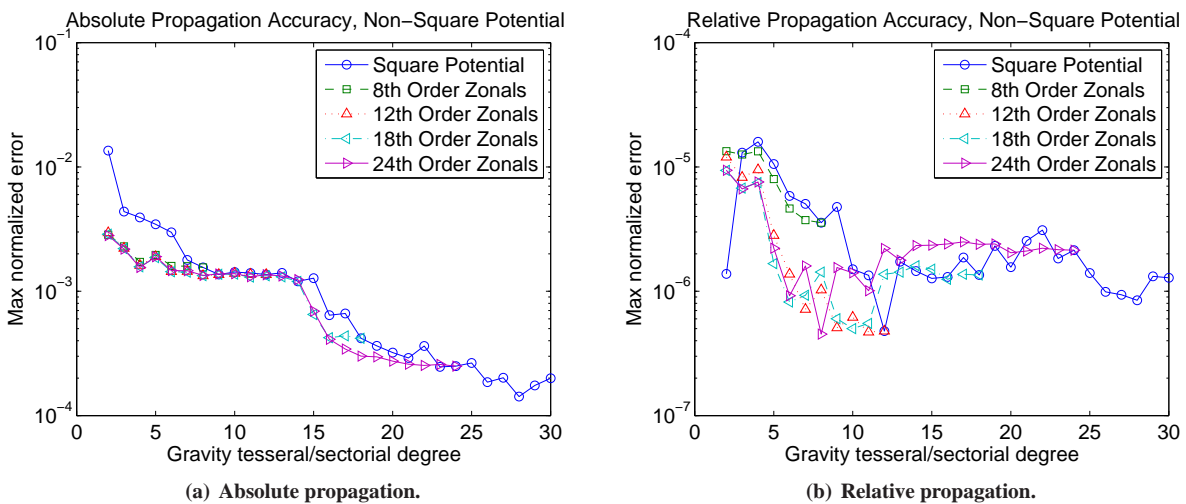


Fig. 6. Comparison of propagation accuracy for non-square geopotential fields.

5. CONCLUSION

In the 400 km–700 km LEO regime with inclinations from 40° – 140° , the most important forces affecting propagation accuracy were found to be the J_2 Earth oblateness and atmospheric drag, followed by higher order geopotential terms, from an overall order of magnitude perspective. Forces were compared over a very long time span in terms of a combination of position and speed (not velocity) errors for both absolute and relative results. The impact of drag on relative accuracy is insignificant when the spacecraft have the same cross-sectional area and differential drag is negligible. In general, when differential drag is small, the relative propagation accuracy is very good and there is little improvement with higher-order gravity models. For absolute propagation, when drag is not included in the force model, there is little increase in accuracy for gravity models larger than 3×3 . For both absolute and relative propagation, when drag is included, there is a general improvement in accuracy for gravity fields of order/degree higher than 2×2 , but the improvement is not monotonic and there is no clear “best” gravity model truncation. Altitude and inclination influence the results because of their impact on drag: they determine how dense of an atmosphere the spacecraft will travel through, which determines the magnitude of the drag force. Drag effects are greater at lower altitudes and near-equatorial inclinations than at higher altitudes and near-polar inclinations. Lunar and solar third-body perturbations and solar radiation pressure did not have a significant effect on propagation accuracy in this regime, compared to Earth gravity and drag.

A more detailed, 1 day propagation was analyzed for a 425 km Sun-synchronous orbit (the current baseline for PONSFD) with mild differential drag and errors in both atmospheric density modeling and attitude knowledge. These errors have a significant impact on absolute and relative propagation and demonstrate that if drag modeling is to be beneficial at all it is essential to characterize these parameters accurately. It was also shown that truncation of the zonal terms in the geopotential has more of an impact on propagation accuracy than truncation of the tesseral and sectorial terms for both the absolute and relative results. However, the 15th and 16th degree tesseral/sectorial terms are quite important for very high accuracy applications in this particular orbit. Therefore, in evaluating a trade-off between gravity model complexity and computational processing requirements, it would be wise to increase the order of the zonal terms and retain lower degree tesseral/sectorial terms rather than restricting attention to a square geopotential.

6. ACKNOWLEDGMENTS

The authors wish to thank Scott MacGillivray, Ai Tsuda, and John Bowen of Tyvak Nano-Satellite Systems LLC for their support and technical input to this work. We also appreciate the advice of David Vallado, who helped us understand some of the issues and history of gravity model truncation. Finally, we thank Christopher O'Hare for his assistance in the preparation of this manuscript.

REFERENCES

- [1] D. Brouwer, "Solution of the Problem of Artificial Satellite Theory Without Drag," *The Astronomical Journal*, Vol. 64, November 1959, pp. 378–397.
- [2] W. N. Barker, S. J. Casali, and R. N. Wallner, "Earth Gravitational Error Budget for Space Control," *Advances in the Astronautical Sciences*, Vol. 93, 1996, pp. 351–370. (Proceedings of the AAS/AIAA Spaceflight Mechanics Meeting, Austin, TX, February 12–15 1996).
- [3] J. E. Register, "Contributions of Individual Forces to Orbit Determination Accuracy," *Advances in the Astronautical Sciences*, Vol. 114, 2003, pp. 1819–1838. (Proceedings of the AAS/AIAA Spaceflight Mechanics Meeting, Ponce, Puerto Rico, February 9–13 2003).
- [4] D. A. Vallado, "An Analysis of State Vector Propagation Using Differing Flight Dynamics Programs," *Advances in the Astronautical Sciences*, Vol. 121, 2005. (Proceedings of the 15th AAS/AIAA Space Flight Mechanics Meeting, Copper Mountain, CO, January 23–27 2005).
- [5] D. A. Vallado, *Fundamentals of Astrodynamics and Applications*. Hawthorne, CA: Microcosm Press, 3rd ed., 2007.
- [6] D. A. Vallado and D. Finkleman, "A Critical Assessment of Satellite Drag and Atmospheric Density Modeling," *AIAA/AAS Astrodynamics Specialist Conference and Exhibit*, Honolulu, HI, August 18–21 2008.
- [7] J. R. Carpenter and K. T. Alfriend, "Navigation Accuracy Guidelines for Orbital Formation Flying," *AIAA Guidance, Navigation, and Control Conference and Exhibit*, Austin, TX, August 11–14 2003.
- [8] C. Sabol, R. D. Burns, and C. A. McLaughlin, "Satellite Formation Flying Design and Evolution," *Journal of Spacecraft and Rockets*, Vol. 38, March–April 2001, pp. 270–278.
- [9] E. Wnuk and J. Golebiewska, "The Relative Motion of Earth Orbiting Satellites," *Celestial Mechanics and Dynamical Astronomy*, Vol. 91, March 2005, pp. 373–389.
- [10] C. C. Romanelli, A. Natarajan, H. Schaub, G. G. Parker, and L. B. King, "Coulomb Spacecraft Voltage Study due to Differential Orbital Perturbation," *Advances in the Astronautical Sciences*, Vol. 124, 2006, pp. 361–380. (Proceedings of the 16th Space Flight Mechanics Meeting, Tampa, FL, January 22–26 2006).
- [11] S. P. Hughes, "Formation Design and Sensitivity Analysis for the Magnetospheric Multiscale Mission (MMS)," *AIAA/AAS Astrodynamics Specialist Conference*, Honolulu, HI, August 18–21 2008.
- [12] C. W. T. Roscoe, S. R. Vadali, and K. T. Alfriend, "Third-Body Perturbation Effects on Satellite Formations," *Advances in the Astronautical Sciences*, Vol. 147, 2013, pp. 483–502. (Proceedings of the Jer-Nan Juang Astrodynamics Symposium, College Station, TX, June 24–26 2012).
- [13] S. D'Amico, J.-S. Ardaens, and O. Montenbruck, "Navigation of Formation Flying Spacecraft using GPS: the PRISMA Technology Demonstration," *ION-GNSS-2009*, Savannah, GA, September 22–25 2009.
- [14] R. J. Suggs, "Future Solar Activity Estimates for Use in Prediction of Space Environmental Effects on Spacecraft Orbital Lifetime and Performance," tech. rep., NASA Marshall Space Flight Center, March 2013.